J Korean Med Sci 1999; 14: 502-10
ISSN 1011-8934

Percutaneous Transmyocardial Revascularization Induces Angiogenesis: A Histologic and 3-Dimensional Micro Computed Tomography Study

The purpose of this study was to visualize the spatial patterns and connection of channels created after percutaneous transmyocardial revascularization (PTMR) in normal porcine hearts, and to estimate the relative contributions of transmyocardial and coronary perfusion. Six pigs underwent PTMR creating channels using radiofrequency ablative energy. Three-dimensional computed tomography imaging of channels 1 hr after PTMR showed the direct connection of PTMR channels to the myocardial capillary network and to epicardial coronary vessels. In the heart, examined 28 day after PTMR, there was a fine, extensive, network of microvessels originating from the site of the original PTMR channel, also connecting the left ventricular cavity to myocardial capillaries. Histopathologic examination of the 1-hr specimens showed numerous regions of myocardial hemorrhage and associated inflammatory cell infiltration. In the 28-day specimens, newly developed new vascular network suggested neovascularization within the core of these channel remnants. The immunoreactivity for basic fibroblast growth factor (bFGF) and vascular endothelial growth factor (VEGF) were intense within myocardium and neovascular structure surrounding PTMR channel remnants. The vascular connections occur by direct communication with existing myocardial vasculature acutely, and angiogenesis in these channel remnant chronically.

Key Words: *Myocardial revascularization; Neovascularization, physiologic; Angiogenesis factor*

Hyuck Moon Kwon, Bum Kee Hong, Gil Jin Jang, Dong Soo Kim, Eui Young Choi, In Jai Kim, Charles J. McKenna*, Eric L. Ritman†, Robert S. Schwartz*

Department of Internal Medicine, Yong-Dong Severance Hospital, Yonsei University College of Medicine, Seoul, Korea
*The Division of Cardiovascular Diseases, and †the Department of Physiology and Biophysics, Mayo Clinic and Mayo Foundation, Rochester, MN. U.S.A.

Received: 13 April 1999
Accepted: 18 May 1999

Address for correspondence
Hyuck Moon Kwon, M.D.
Cardiology Division, Department of Internal Medicine, Yong-Dong Severance Hospital, Yonsei University College of Medicine, Yongdong P.O. Box 1217, Seoul 135-720, Korea
Tel: +82.2-3497-3310, Fax: +82.2-573-0112
E-mail: kwonhm@yumc.yonsei.ac.kr

INTRODUCTION

Surgical transmyocardial revascularization (TMR) using epicardial laser has generated much interest as a therapy to relieve angina in selected patients (1, 2). However, enthusiasm for this treatment modality has recently been stimulated by clinical studies demonstrating improved symptomatology and reduced number of reversible perfusion defects in patients with severe angina who have undergone the TMR procedure (3-10).

Many aspects of TMR remain unclear. A central question concerns the blood vessel connections that develop after TMR channel creation, and whether such channels connect to the left ventricular cavity in both acute and chronic settings (11-17). Perfusion in these channels remains uncertain, as early reports showed no evidence of myocardial perfusion through acute TMR channels using microsphere injection (5, 18-22). Another key question relates to whether the method of channel creation affects neovascularization and long-term patency. Some studies suggest myocardial protection using needle-produced myocardial channels compared with laser TMR (23), others indicate that laser energy may result in better patency by causing less thrombosis (24, 25).

In this study, we examined PTMR with two principal questions in mind: 1) dose non-penetrating, that is whether non-transmural radiofrequency PTMR induces neovascular formation and if so, 2) what are the acute (1 hr) and chronic (28 days) connections of the vasculature using this approach?

To address these questions, we created a catheter-based radiofrequency PTMR from the endocardial left ventricular cavity surface in normal porcine myocardium. The aims of this study was to visualize and quantitate the spatial patterns of channels created after PTMR in normal porcine myocardium using a microscopic three-dimensional (3D) computed tomography imaging technique (26). We compared acute with chronic histologic fea-

tures in the porcine myocardium following PTMR, and performed immunochemistry for neovascularization.

MATERIALS AND METHODS

Animals

Juvenile, domestic crossbred swines three-four months old were fed a normal laboratory chow diet. Ketamine (30 mg/kg body weight) and Xylazine (3 mg/kg) were given intramuscularly for general anesthesia. Atropine (1 mg) was used intramuscularly to decrease oropharyngeal secretions and Flocillin (1 g) was given as a prophylaxis against infection. Arterial access was obtained through carotid arterial cut-down after infiltration of the ventral neck region with 10 mL of 1% Xylocaine. The right external carotid artery was exposed and a 9F hemostatic sheath placed for arterial access. A single heparin bolus of 10,000 units was administered through the sheath. The carotid arteriotomy was repaired with standard techniques or ligated if repair was not possible. The neck wound was closed with interrupted sutures and the animals were returned to their quarters for observation. Pigs survived either 1 hr or 28 days. The animals were euthanized with an intravenous commercial euthanasia solution (Sleepaway, Fort Dodge Laboratory).

Radiofrequency PTMR procedure

Catheter-based endocardial TMR was performed in six pigs using ablative radiofrequency (RF) energy for non-transmural channel creation. This device consisted of a 1 mm guide wire insulated up to but not including the very distal tip. A mechanical collar on this electrode prevented tissue penetration of more than 7 mm depth. For tissue ablation, the device was energized with a standard electrosurgical generator (Valleylab Inc, Boulder, Colorado, U.S.A.) and operated as below.

A 9 Fr guide catheter was placed retrogradely across the aortic valve into the ventricle using a soft 0.035 guide wire. The PTMR electrode was advanced through the catheter into the left ventricle and positioned perpendicularly against the anterior free wall. The device was then attached to the RF generator and activated using a foot switch. Each depression of the foot pedal resulted in one second pulse of pure sine wave energy (450 Khz) to the electrode. The power delivered to the electrode was between 15-20 watts during ablation. Five to ten channels were created in each pig heart at a spatial density of about one per square centimeter. Each channel was approximately 7 mm deep and 1 mm in diameter. Following creation of all channels, the device was then removed, the access vessel repaired and the animal were returned to quarters.

Histopathologic analysis

Histologic sections were reviewed from one-hr (n=3, acute) and 28-day (n=3, chronic) pigs. All myocardial specimens (porcine and patient) were paraformaldehyde fixed, after which the treated myocardial segments were dissected free and cut at 2 mm intervals. The tissues were subsequently wax embedded and stained with hematoxylin-eosin or methylene blue.

Myocardial block preparation, coronary artery perfusion and polymer injection

The porcine hearts were perfusion fixed under a pressure of 70 mmHg for 24 hr. Two blocks of the PTMR-treated porcine myocardium (2 cm×2 cm, grossly identified from the endocardial side) were chosen at random from each heart, removed and scanned for 3-dimensional reconstruction images as follow.

In the one-hr specimens, a 24 gauge soft and flexible polyethylene cannula was introduced into the left ventricular orifice of endocardial channels. A specially prepared low viscosity, radiopaque liquid polymer compound (MV-122, Canton Biomedical Products, Boulder, Colorado) was then injected through the cannula at a pressure of 40 mmHg, to determine the myocardial microvascular area supplied via the TMR channels. This polymer hardened when the myocardial blocks were placed under refrigeration at 4℃ overnight. On the following day, the blocks were placed in 95% alcohol for 48 hr. At successive 24 hr intervals, the glycerin concentration was raised to 35, 50, 75% and, finally, pure glycerin for purposes of dehydration. Next, the myocardial blocks were rinsed with acetone and left in open air for 24 hr. The myocardial blocks were then rinsed with acetone and left to dry in air for 24 hr. The blocks were then embedded in a paraffin mold for scanning and 3D micro-CT imaging.

In two normal (control) porcine hearts not subjected to PTMR, glass cannulae were tied at the coronary orifices and injected with 500 mL of heparinized saline (0.9% sodium chloride with 2,000 units of heparin) at a pressure of 70 mmHg to clear the coronary network of remaining blood. The same low viscosity, radiopaque polymer compound was then injected through the cannulae and the hearts prepared as above. The purpose of this preparation was to observe myocardial microvascular patterns in normal hearts as it occurs by the epicardial coronary route. Subendocardial vascular area by the epicardial coronary route could then be compared with the

PTMR-treated subendocardial vascular area, to calculate the ratio (%) of PTMR to normal coronary vascular area.

Microscopic three-dimensional and cross-sectional CT

Myocardial blocks were scanned by a novel micro-CT system consisting of a spectroscopy X-ray tube, a fluorescent crystal plate, a microscopic objective and a charge coupled device (CCD) camera for imaging (26-28). Briefly, a specimen is rotated in the X-ray beam, resulting in 500-1,000 projections during a 360 degree rotation. Three dimensional images were reconstructed using a modified Feldkamp cone beam filtered back projection algorithm and the resulting 3-dimensional images were displayed using Mayo Analyze software (Version 7.5, Biomedical Imaging Resource, Mayo Foundation). In this study, volume rendering provided a variety of display representations of three-dimensional image data sets. Volume rendered-transmission displays, voxel gradient shading and maximum intensity projection were displayed at various angles and threshold values of voxels. Average voxel size was 21-25 μm, and images of up to 800 slices were rendered for each myocardial block (each with a matrix 10-20 μm cubic voxels $\times$ 16 bits of gray scale). Five to seven cross-sectional images, every 2 mm, were analyzed from each myocardial block at a pixel size of 25 μm.

All cross-sectional images were shown from endocardium to epicardium, which included the PTMR-treated orifice and epicardial coronary arteries and veins. The inner half thickness of myocardium near to the endocardial PTMR was defined as subendocardium and the outer half near to epicardium was defined as subepicardium. The polymer filled blood vessels within these boundaries were defined as subendocardial, excluding the PTMR channels, or subepicardial, excluding epicardial coronary arteries/veins. The microvasculature area in the subepicardium or subendocardium was differentiated from non-vascular structures by setting the lower threshold values for an intensity range of interest that yielded the best identification of microvasculature regions as judged by two independent observers. The microvasculature area in the subendocardial region was determined by computer, summed and divided by the subendocardial area. Hence, the values for summed subendocardial microvasculature area/total subendocardium area (%), as indices of normal coronary and PTMR-created neovascular area, were calculated.

Immunohistochemistry

Paraffin sections (5 μm) were made and transferred to glass slides. Slides were deparaffinized and rehydrated through the following solutions: xylene twice for 5 min, 100% ethanol twice for 10 dips and 95% ethanol twice for 10 dips. Endogenous peroxidase activity was blocked for 10 min at room temperature in 50% volume H_2O_2/ 50% volume methanol and rinsed in running tap water. Non-specific protein binding sites were blocked by applying 5% normal goat serum diluted in PBS/0.05% Tween 20 (pH=7.2-7.4) to slides for 10 min at room temperature. The serum was blotted off and the primary antibody (mouse anti-human bFGF, Calbiochem, San Diego, CA, U.S.A., or anti-human VEGF monoclonal antibody, Sigma, St. Louse, MO, U.S.A.) was diluted in 1% normal goat serum+PBS/0.05% Tween 20, applied and incubated overnight at 4℃ in a humidity chamber. On day 2, the primary antibody was rinsed off in tap water, then blotted. The biotinylated secondary antisera cocktail (including goat anti mouse IgG and goat anti rabbit) dilution was incubated on the slides for 30 min at room temperature. Slides were rinsed in running tap water, blotted and streptavidin-horseradish peroxidase was diluted 1/400 in PBS/0.05% Tween 20+1% normal goat serum was applied and incubated for 30 min at room temperature. The slides were rinsed in tap water and color developed in 3-amino-9-ethylcarbazole substrate solution for 15 min at room temperature, counterstained in hematoxylin for 30 sec and coversliped.

Stock solutions

Tween 20	Pierce Chemical Co
Normal Goat Serum	Dako (Carpinteria, CA, U.S.A.)
Biotinylated Mouse IgG	Dako
Biotinylated Rabbit IgG	Dako
Streptavidin-horseradish peroxidase	Dako
3-amino-9-ethycarbasole	Sigma (St Louis, MO, U.S.A.)

RESULTS

Histopathologic analysis and microscopic 3-D CT imaging

Fig. 1 shows the histologic and micro-CT images of normal myocardium perfused antegrade by epicardial coronary arteries. It appears the highly vascular nature of the normal porcine heart is well demonstrated. Fig. 2 shows PTMR-treated porcine myocardium 1 hr after the procedure. These images demonstrate direct connection between the new PTMR channels, the left ventricular cavity and the preexisting coronary vessels. Oblique, two dimensional cross sectional images in the plane of the PTMR channel showed contrast material and presumably blood having dissected into the myocardium in the peri-

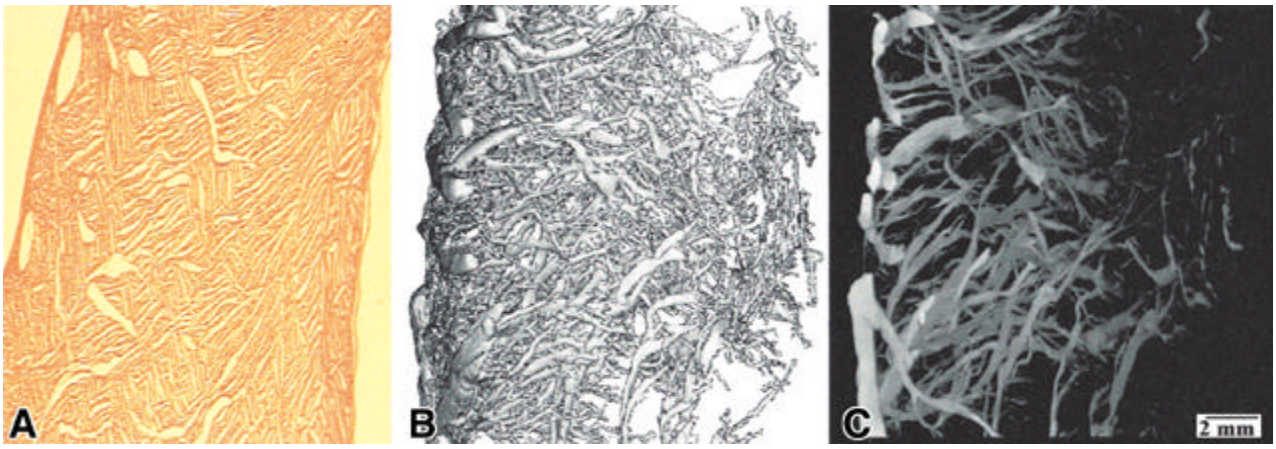

Fig. 1. Histologic section (H-E, ×12.5, A), voxel gradient shading (B) and maximum intensity projection (C). These are three-dimensional images of normal porcine myocardium perfused antegrade by epicardial coronary arteries. The highly vascular, capillary rich nature of the heart is readily appreciated. Voxel size 30 m.

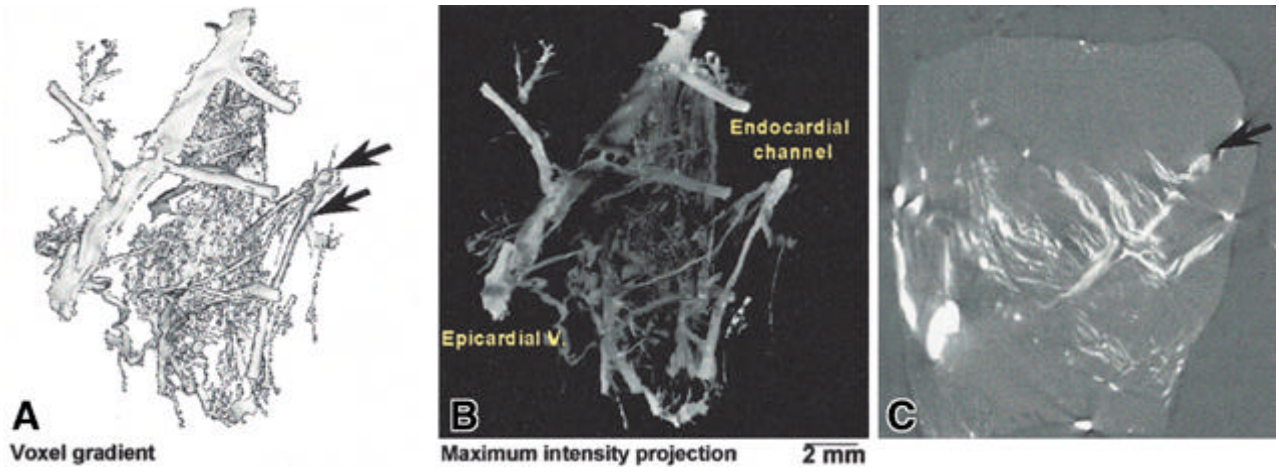

Fig. 2. Voxel gradient shading (A) and maximum intensity projection (B) from a porcine myocardial block 1 hr following PTMR treatment. Three-dimensional reconstruction demonstrates direct connection of the PTMR channel (arrow) with preexisting coronary vessels. Voxel size 30 m. Transverse cross-sectional images of porcine myocardium injected with liquid polymer 1 hr (C) through patent PTMR channel. Acutely following PTMR, the treatment sites were surrounded by blood-filled spaces. These suggest extensive intramyocardial hemorrhage.

channel region. This suggests intramyocardial hemorrhage at this early time point (Fig. 2C). Histopathologic examination of myocardium at 1 hr demonstrated that open PTMR channels (Fig. 3A) and thrombosed PTMR channels (Fig. 3B) were surrounded by blood-filled intramyocardial hemorrhage regions. Additionally, these sections had associated inflammatory cell infiltration originating from PTMR cannel sites (Fig. 3C, D).

At 28 days, the PTMR-treated myocardium showed an extensive network of capillaries in the endocardium at the site of PTMR channel creation in the left ventricular wall. These capillaries were similarly connected with the preexisting coronary vessels (Fig. 4). No patent channel was identified, grossly or microscopically. All original channels were replaced with granulation tissue and fibrosis, referred to as the channel remnant. In these 28-day specimens, newly developed new vascular network suggested neovascularization under the base of granulation tissue (Fig. 5A, B). Because some of these channels were sectioned at slightly different angles, the cross sections were elliptical. Microscopically, the typical appearance of channel remnant showed an oblique fibrous scar confirmed by trichrome stain (Fig. 5B). There were also no obvious differences between PTMR channels on gross examination.

Porcine histopathology at 28 days following PTMR was analyzed with stained sections and immunoreactivity for the bFGF and VEGF. In 28 days, following PTMR, the myocardial tissue, especially subendocardium, showed a highly vascularized scar at site of previous channels cre-

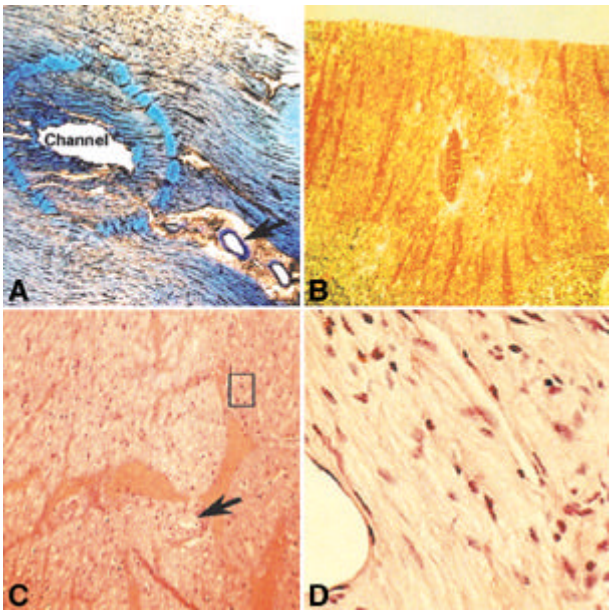

Fig. 3. Acute histologic images of porcine myocardium following PTMR. A: Central channel region was surrounded by small tissue necrosis (methylene blue, ×40). B: A channel was thrombosed and surrounded by blood-filled spaces (H-E, ×40). C: It shows numerous regions of myocardial hemorrhage (H-E, × 40), with an associated inflammatory cell infiltrate (D, ×400), originating from channel sites. Arrows indicate the preexisting coronary vessel.

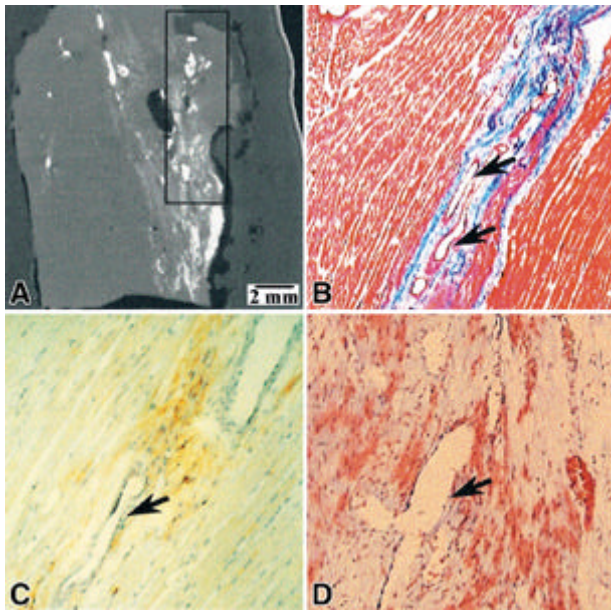

Fig. 5. Transverse cross-sectional images of porcine myocardium injected with liquid polymer 28 days (A) following PTMR treatment. Chronically, there is highly vascular subendocardial filling at the site of previous channel creation. (B) Central channel region is replaced by granulation tissue, fibrosis and new vessel formation (Trichrome, ×40). Arrows indicate new vessel formation. Immunohistochemical stainings for the VEGF (C) and bFGF (D). Immunoreactivity for the bFGF and VEGF were intense within the neovascular structure of the granulation tissue surrounding PTMR channel remnants (×100).

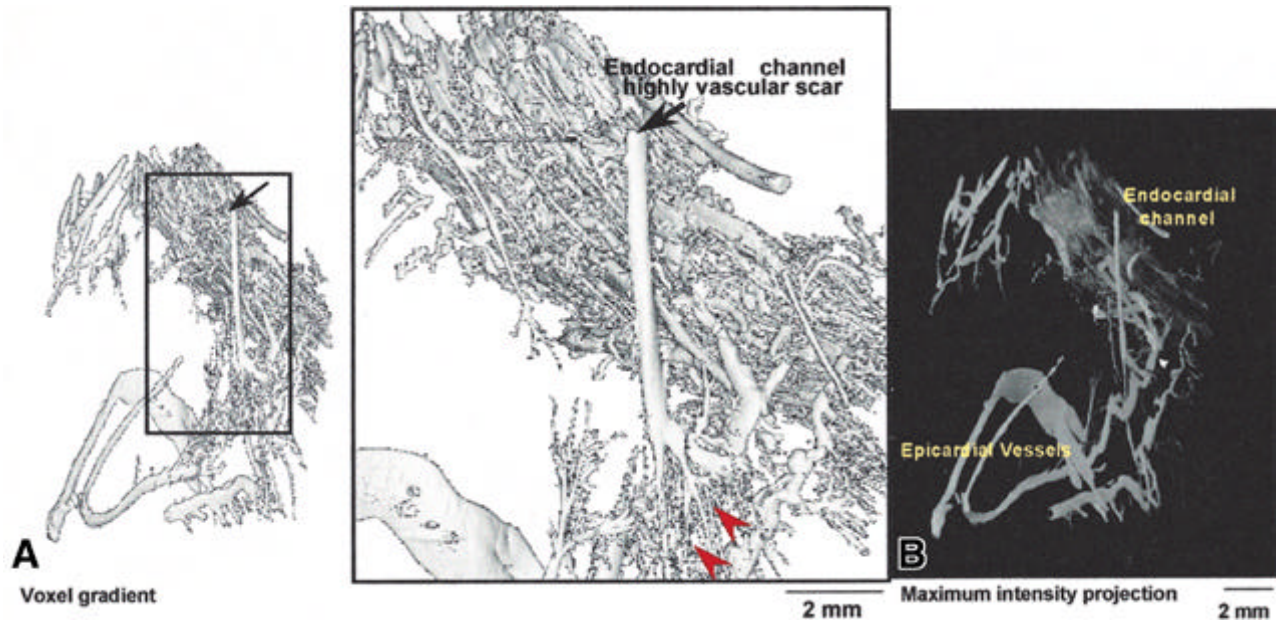

Fig. 4. Voxel gradient shading (A) and maximum intensity projection (B) from a porcine myocardial block 28 days following endocardial PTMR. An extensive subendocardial microvascular network (box area) can be seen originating from the site of replaced with granulation tissue and fibrosis, referred to as the channel remnant (arrow) and interconnecting with preexisting coronary vessels. Voxel size 30 m. Arrow head indicate angiogenesis from channel remnant.

Table 1. Microvascular contrast as a percentage of myocardium: Epicardial coronary artery filling vs. PTMR at 1 hr and 28 days

	Coronary (n=25)	PTMR at 1 hr (n=24)	PTMR at 28 days (n=29)
Microvascular area	33.72.5%	13.61.0%*	20.41.7%*

*$p<0.05$ compared with coronary artery contrast injection

ation. We also examined the immunolocalization of bFGF and VEGF in the normal myocardium surrounding PTMR channel remnants. Immunoreactivity for the bFGF and VEGF were intense within the neovascular structure of the granulation tissue surrounding PTMR channel remnants (Fig. 5C, D).

Digital quantitation of the cross-sectional images

Cross-sectional images containing the PTMR channels were measured to estimate the fraction of myocardium occupied by microvasculature as vascular area/tissue area (%). These measurements were made for normal myocardium which was filled by antegrade coronary artery polymer injections, and compared with the separate myocardium that underwent PTMR both 1 hr and 28 days prior to euthanasia. Multiple regions were sampled in each segment of myocardium (Table 1). In performing this measurement, voxels with intensity corresponding to microvasculature were counted automatically by computer, and divided by the total myocardial voxel area of the sub-region measured. The microvasculature area/total myocardial area (vascular area/tissue area) for coronary filled subendocardium was 33.7%±2.5%. This compared with 13.6%±1.0% for 1 hr post PTMR and 20.4 %±1.7% for 28 days post PTMR (Table 1).

DISCUSSION

Since the introduction of transmyocardial revascularization, many questions remain unanswered regarding its efficacy and the role of myocardial channels. In a recent clinical trial of laser TMR, 75% of surviving patients experienced a decrease of two functional anginal classes, and 56% decreased their use of anti-anginal medications at 10 months follow-up. Moreover, objective measurement of left ventricular radionuclide perfusion defects before and after TMR showed significantly fewer segments with reversible defects both 6 and 12 months after treatment. Patients imaged by positron emission tomography (PET) scannning showed improved subendocardial perfusion in treated areas at 12 months (9). While these clinical data are encouraging, an understanding of the basic mechanism is lacking.

Thus, we undertook the present study to better understand the anatomic nature and connections of the PTMR channels. There were two major findings of the present study. First, percutaneous, non-transmural radiofrequency channels do result in angiogenesis occurring in the PTMR scar. And second, this microvasculature connects the left ventricular cavity to myocardial capillaries and epicardial coronary arteries and veins, both acutely and chronically. In normal porcine myocardium, these connections occurred within an 8 cubic centimeter myocardial block. This information may be useful in determining required distances between channels for therapeutic clinical response. This surprisingly large region of microvasculature connections suggests that the number of channels needed may be less than that obtained from the 20-30 channels presently employed. Reducing the number of channels created per patient might shorten the procedure and potentially increase its safety.

This study also found very similar histopathologic results after endocardial PTMR in porcine myocardium compared with patients treated by epicardial laser PTMR. Acutely, there was intramyocardial hemorrhage and an associated inflammatory cell infiltration. Chronically, mature arterial vessels frequently existed within the core of these channel remnants under the base of granulation tissue or fibrosis, connecting to the intramyocardial capillaries and epicardial coronary vessels. These findings suggest that the mechanism of channel creation (radiofrequency or laser) may not alter the final result of angiogenesis. Angiogenesis in transmyocardial revascularization may also reveal similar angiogenic process of non-myocardial wound healing.

This was an anatomic study, and did not evaluate perfusion. However, myocardial perfusion might occur acutely after non-transmural endocardial channel creation, through the communications we found between existing myocardial vasculature and the PTMR channels. This is consistent with increased subendocardial myocardial perfusion demonstrated on the PET scans in patients treated with epicardial laser TMR (9). Anecdotal reports of patients treated with laser PMR similarly suggest early anginal relief after the procedure. Similarly, chronic perfusion might occur by the microvessels of the chronic scar and its connections to the myocardium.

These findings are in agreement with findings by Cooley et al. (29). This study found connections between the left ventricular cavity and intramyocardial sinusoids

at three months, and suggested that TMR can acutely revascularize the myocardium. The initial sinusoidal connections were thought to enlarge and become direct arteriolar channels when exposed to a significant pressure gradient (30). Similar sinusoids of the reptilian heart form an important source of myocardial blood supply in reptilian hearts (31), but their role in humans is not fully understood.

Another study used an endocardial approach and demonstrated that blood penetrated the myocardial wall directly through channels made with a pulsed Ho:YAG laser in the acute setting (31). Although the neovascularization was found later around these channels, flow into the left ventricular chamber could not be demonstrated after two weeks using microsphere analysis.

There is contradictory evidence from studies measuring blood flow that TMR channels fail to provide blood to surrounding myocardium in the first few hours (5, 13, 16). Hardy used a CO_2 laser TMR in dogs following coronary artery ligation and found that regional blood flow was increased only when combined with elevated left ventricular pressure (13). Following TMR channel creation, red blood cells were shown in this study to enter intramyocardial coronary tributaries, taking the path of least resistance. These investigators postulated that new channels might connect with postcapillary veins, thereby directing blood flow retrograde through capillaries and improving myocardial perfusion. This is in essence what we observed acutely following non-transmural PTMR in normal porcine heart. Non-transmural PTMR may drive blood toward endocardial channels in the acute setting. These channels may communicate with intramural arteriolar and venular networks.

Our study examined normal porcine hearts, similar to prior experimental work (32-34). The endocardial and epicardial surfaces of the pig heart contain arcading veins, but not arteries, which connect with thebesian and sinusal veins, respectively. The thebesian and sinusal veins communicate with each other through venous anastomoses. The coronary venous system also demonstrates sinusoidal patterns, with dense networks of vessels draining into them. Coronary artery stenosis causes retrograde perfusion through the coronary veins (35). With retrograde perfusion pressure, blood is shunted from capillaries through lower resistance anastomoses. As retrograde pressure increases, epicardial and eventually transmural capillary filling occurs. This is one possible mechanism whereby the non-transmural endocardial channel may improve perfusion in the porcine model. However, such anatomic structure and communication is yet to be defined in normal human myocardium.

Evidence suggests that the repair process initiated by this type of myocardial injury results in the formation of new functioning vasculature (36-44). This hypothesis suggests that inflammatory and thrombotic reactions to injury cause local release of mediators (substance P, thrombin, histamine, tryptase) and endogenous vasodilators (nitric oxide, adenosine). These mediators and vasodilators, in turn, stimulate the production of vascular growth factors (bFGF, VEGF) which subsequently promote endothelial cell proliferation and angiogenesis. It is likely that the communicating network created acutely by TMR forms a nidus for subsequent thrombus formation, inflammation and future angiogenesis. This evidence has been derived from observations made in experimental tissue that many, apparently new, blood vessels appear within the granulation tissue that invades the original channels (i.e., neovascularization within the channel remnants) (45, 46). Such observations, however, provide limited support for the angiogenesis hypothesis because blood vessels within scar tissue by themselves may not contribute meaningfully to myocardial perfusion. In the present study, we showed that by 28 days after creating endocardial PTMR channels in normal porcine hearts active vascular growth in the normal myocardium surrounding PTMR channel remnants occurs.

In conclusion, this study used microscopic 3-dimensional CT imaging in normal and PTMR-treated porcine myocardium. Two principal conclusions resulted. First, this study provides a unifying hypothesis about potential mechanisms whereby PTMR may improve ischemic myocardium. Acutely, the PTMR channels create a network of blood-filled spaces within the myocardium. These channels initially connect to the myocardial capillaries, which in turn connect to the epicardial coronary arteries and veins. Chronically, these spaces may act as a nidus for thrombus formation. Thrombus, and the trauma of channel creation stimulate inflammation, with release of mediators promoting angiogenesis. Chronically, microvascular channels grow and improve myocardial perfusion even though created channels are occluded with scar tissue or organized thrombus.

The second conclusion is that channels in porcine myocardium using ablative radiofrequency energy showed very similar acute and chronic histopathology to lesions from patients treated with laser TMR. This implies that laser is not an essential component of the angiogenesis that follows the healing of the channels. Second, no channels remained patent in the context of a blood-filled cavity the size of the PTMR electrode. Instead, the channels healed with a highly vascular scar at the site of the channel creation.

Whether TMR or PTMR become widely used as a clinical therapy is uncertain. Regardless, it is crucial that we understand the anatomy and physiology of myocardial angiogenesis and perfusion following channel creation.

REFERENCES

1. Sen PK, Daulatram J, Kinare SG, Udwadia TE, Parulkar GB. *Further studies in multiple transmyocardial acupuncture as a method of myocardial revascularization. Surgery 1968; 64: 861-70.*
2. White M, Hershey JE. *Multiple transmyocardial puncture revascularization in refractory ventricular fibrillation due to myocardial ischemia. Ann Thorac Surg 1968; 6: 557-63.*
3. Goda T, Wierzbicki Z, Gaston A, Leandri J, Vouron J, Loisance D. *Myocardial revascularization by CO_2 laser. Eur Surg Res 1987; 19: 113-7.*
4. Mirhoseini M, Shelgikar S, Cayton MM. *New concepts in revascularization of the myocardium. Ann Thorac Surg 1988; 45: 415-20.*
5. Landreneau R, Nawarawong W, Laughlin H, Ripperger J, Brown O, McDaniel W, McKown D, Curtis J. *Direct CO_2 laser revascularization of the myocardium. Lasers Surg Med 1991; 11: 35-42.*
6. March RJ, Guynn T. *Cardiac allograft vasculopathy: the potential role for transmyocardial laser revascularization. J Heart Lung Transplant 1995; 14(suppl): 242-6.*
7. Horvath KA, Mannting F, Cummings N, Shernan SK, Cohn LH. *Transmyocardial laser revascularization: operative techniques and clinical results at two years. J Thorac Cardiovasc Surg 1996; 111: 1047-53.*
8. Cooley DA, Frazier OH, Kadipasaoglu KA, Lindenmeir MH, Pehlivanoglu S, Kolff JW, Wilansky S, Moore WH. *Transmyocardial laser revascularization: clinical experience with twelve-month follow-up. J Thorac Cardiovasc Surg 1996; 111: 791-9.*
9. Horvath KA, Cohn LH, Cooley DA, Crew JR, Frazier OH, Griffith BP, Kadipasaoglu K, Lansing A, Mannting F, March R, Mirhoseini MR, Smith C. *Transmyocardial laser revascularization: results of a multicenter trial with transmyocardial laser revascularization used as sole therapy for end-stage coronary artery disease. J Thorac Cardiovasc Surg 1997; 113: 645-54.*
10. Malik FS, Mehra MR, Ventura HO, Smart FW, Stapleton DD, Ochsner JL. *Management of cardiac allograft vasculopathy by transmyocardial laser revascularization. Am J Cardiol 1997; 80: 224-5.*
11. Pifarre R, Jasuja ML, Lynch RD, Neville WE. *Myocardial revascularization by transmyocardial acupuncture: a physiologic impossibility. J Thorac Cardiovasc Surg 1969; 58: 424-31.*
12. Walter P, Hundeshagen H, Borst HG. *Treatment of acute myocardial infarction by transmural blood supply from the ventricular cavity. Eur Surg Res 1971; 3: 130-8.*
13. Hardy RI, James FW, Millard RW, Kaplan S. *Regional myocardial blood flow and cardiac mechanics in dog hearts with CO_2 laser-induced intramyocardial revascularization. Basic Res Cardiol 1990; 85: 179-97.*
14. Jeevanandam V, Auteri JS, Oz MC, Watkins J, Rose EA, Smith CR. *Myocardial revascularization by laser-induced channels. Surg Forum 1991; 56: 46-53.*
15. Yano OJ, Bielefeld MR, Jeevanandam V. *Prevention of acute regional ischemia with endocardial laser channels. Ann Thorac Surg 1993; 56: 46-53.*
16. Wittaker P, Kloner RA, Przyklenk K. *Laser-mediated transmural myocardial channels do not salvage acutely ischemic myocardium. J Am Coll Cardiol 1993; 22: 302-9.*
17. Horvath KA, Smith WJ, Laurence RG, Schoen FJ, Appleyard RF, Cohn LH. *Recovery and viability of an acute myocardial infarct after trnasmyocardial laser revascularization. J Am Coll Cardiol 1995; 25: 258-63.*
18. Yano OJ, Bielefeld MR, Jeevanandam V, Treat MR, Marboe CC, Spotnitz HM, Smith CR. *Prevention of acute regional ischemia with endocardial laser channels. Ann Thorac Surg 1993; 56: 46-53.*
19. Kohmoto T, Fisher PE, Gu A, Zhu SM, Yano OJ, Spotnitz HM, Smith CR, Burkhoff D. *Dose blood flow through Holmium:YAG transmyocardial laser channels? Ann Thorac Surg 1996; 61: 861-8.*
20. Fleischer KJ, Goldschmidt-Clermont PJ, Fonger JD, Hutchins GM, Hruban RH, Baumgartner WA. *One-month histologic response of transmyocardial laser channels with molecular intervention. Ann Thorac Surg 1996; 62: 1051-8.*
21. Burkhoff D, Fisher PE, Apfelbaum M, Kohmoto T, DeRosa CM, Smith CR. *Histologic appearance of transmyocardial laser channels after 4.5 weeks. Ann Thorac Surg 1996; 61: 1532-5.*
22. Hardy RI, Bove KE, James FW, Kaplan S, Goldman L. *A histologic study of laser-induced transmyocardial channels. Lasers Surg Med 1987; 6: 563-73.*
23. Whittaker P, Rakusan K, Kloner RA. *Transmural channels can protect ischemic tissue: assessment of long-term myocardial response to laser- and needle-made channels. Circulation 1996; 93: 143-52.*
24. Frazier OH, Cooley DA, Kadipasaoglu KA, Pehlivanoglu S, Lindenmeir M, Barasch E, Conger JL, Wilansky S, Moore WH. *Myocardial revascularization with laser: preliminary findings. Circulation 1995; 92(suppl): 58-65.*
25. Kim CB, Kesten R, Javier M, Hayese M, Walton AS, Billingham ME, Kernoff R, Oesterle SN. *Percutaneous method of laser transmyocardial revascularization. Cathet Cardiovasc Diagn 1997; 40: 223-8.*
26. Ritman EL, Dunsmuir JH, Faridani A, Finch DV, Smith KT, Thomas PJ. *Local reconstruction applied to x-ray tomography. In: Chavent G, Papanicolaou G, Sack P, Symes W, eds. Volumes in mathematics and its applications: inverse problems in wave propagation. New York, NY: Springer-Verlag, 1997: 443-52.*
27. Avula RTV, Dunsmuir JH, Beighley PE, Thomas PJ, Faridani A, Ritman EL. *A micro-tomographic technique enhanced by a novel image reconstruction algorithm: application to rat coronary vessels [abstract]. FASEB J 1994; 8: 854A.*
28. Flannery BP, Dickman HW, Roberge WG, DAmico KL.

Three-dimensional x-ray micro-tomography. Science 1987; 237: 1439-44.

29. Cooley DA, Frazier OH, Kadipasaoglu KA, Pehlivanoglu S, Shannon RL, Angelini P. *Transmyocardial laser revascularization: anatomic evidence of long-term channel patency. Tex Heart Inst J 1994; 21: 220-4.*
30. Fujita M, Ohno A, Wada O, Miwa K, Nozawa T, Yamanishi K. *Collateral circulation as a maker of the presence of viable myocardium in patients with recent myocardial infarction. Am Heart J 1991; 122: 409-14.*
31. Kohmoto T, Argenziano M, Yamamoto N, Vliet KA, Gu A, DeRosa CM, Fisher PE, Spotnitz HM, Burkhoff D, Smith CR. *Assessment of transmyocardial perfusion in alligator hearts. Circulation 1997; 95: 1585-91.*
32. Kassab GS, Rider CA, Tang NJ, Fung YB. *Morphometry of the pig cornary arterial tree. Am J Physiol 1993; 265: H350-65.*
33. Kassab GS, Lin DH, Fung YB. *Morphometry of the pig cornary venous system. Am J Physiol 1994; 267: H2100-13.*
34. Kassab GS, Fung YB. *Topology and dimensions of the pig capillary networks. Am J Physiol 1994; 267: H319-25.*
35. Oh B, Volpini M, Kambayashi M, Murata K, Rockman HA, Kassab GS, Ross J. *Myocardial function and transmural blood flow during coronary venous retroperfusion in pigs. Circulation 1992; 86: 1265-79.*
36. Folkman J. *Angiogenesis: initiation and control. Ann N Y Acad Sci 1982; 401: 212-27.*
37. Ziche M, Morbidelli L, Masini E, Amerini S, Granger HJ, Maggi CA, Geppetti P, Ledda F. *Nitric oxide mediates angiogenesis in vivo and endothelial cell growth and migration in vitro promoted by substance P. J Clin Invest 1994; 94: 2036-44.*
38. Granger HJ, Ziche M, Howker Jr JR, Meininger CJ, Czisny LE, Zaweja DC. *Molecular and cellular basis of myocardial angiogenesis. Cell Mol Biol Res 1994; 40: 81-5.*
39. Weihrauch D, Arras M, Zimmermann R, Schaper J. *Importance of monocytes/macrophages and fibroblasts for healing of micronecroses in porcine myocardium. Mol Cell Biochem 1995; 147: 13-9.*
40. Krabatsch T, Schaper F, Leder C, Tulsner J, Thalmann U, Hetzer R. *Histological findings after transmyocardial laser revascularization. J Card Surg 1996; 11: 326-31.*
41. Ziche M, Parenti A, Ledda F, DellEra P, Granger HJ, Maggi CA, Presta M. *Nitric oxide promotes proliferation and plasminogen activator production by coronary venular endothelium through endogenous bFGF. Circ Res 1997; 80: 845-52.*
42. Tiefenbacher CP, Chilian WM. *Basic fibroblast growth factor and heparin influence coronary arteriolar tone by causing endothelium-dependent dilation. Cardiovasc Res 1997; 34: 411-7.*
43. Blair RJ, Meng H, Marchese MJ, Ren S, Schwartz LB, Tonnesen MG, Gruber BL. *Human mast cells stimulate vascular tube formation: tryptase is a novel, potent angiogenic factor. J Clin Invest 1997; 99: 2691-700.*
44. Kohmoto T, Fisher PE, Gu A, Zhu SM, DeRosa CM, Smith CR, Burkhoff D. *Physiology, histology, and 2 week morphology of acute transmyocardial channels made with CO_2 laser. Ann Thorac Surg 1997; 63: 1275-83.*
45. Yamamoto N, Kohmoto T, Gu A, DeRosa C, Smith CR, Burkhoff D. *Angiogenesis is enhanced in ischemic canine myocardium by transmyocardial laser revascularization. J Am Coll Cardiol 1998; 31: 1426-33.*
46. Malekan R, Reynolds C, Narula N, Kelley ST, Suzuki Y, Bridges CR. *Angiogenesis in transmyocardial laser revascularization: a nonspecific response to injury. Circulation 1998; 98: II-62-6.*